Extension of the $[(CH_3)_4N]_2MX_4$ family: Phase transitions and lattice parameters of sixteen $[(CH_3)_4Z]_2MX_4$ (Z = P,As,Sb; M = Co,Cu,Zn; X = Cl,Br,I) compounds

Mark R. Pressprich, Marcus R. Bond, and Roger D. Willett
Department of Chemistry, Washington State University, Pullman, Washington 99164
(Received 12 July 1990)

Solid-solid phase-transition temperatures, entropies of transition, and room-temperature lattice parameters of sixteen $[(CH_3)_4Z]_2MX_4$ (Z = P,As,Sb; M = Co,Cu,Zn; X = Cl,Br,I) compounds are reported. $[(CH_3)_4P]_2CoBr_4$, $[(CH_3)_4P]_2CoI_4$, $[(CH_3)_4P]_2ZnBr_4$, $[(CH_3)_4P]_2ZnI_4$, $[(CH_3)_4As]_2CuBr_4$, $[(CH_3)_4As]_2CoI_4$, and $[(CH_3)_4As]_2ZnI_4$ have β-K_2SO_4-type structures, analogous to known $[(CH_3)_4N]_2MX_4$ compounds. Their room-temperature monoclinic space groups correspond to Landau-allowed continuous transitions from a suspected common high-temperature *Pmcn* phase. The associated distortion representations are compatible with X_2 and Z_2 of *Pmcn*. Previously reported $[(CH_3)_4Z]_2MX_4$ (Z = N,P; M = Mn,Fe,Co,Ni,Cu,Zn; X = Cl,Br,I) compounds are also shown to have this compatibility feature for their sub-*Pmcn* phases. The set of compounds $[(CH_3)_4P]_2CoCl_4$, $[(CH_3)_4P]_2ZnCl_4$, $[(CH_3)_4As]_2CuCl_4$, $[(CH_3)_4Sb]_2CoCl_4$, $[(CH_3)_4Sb]_2CuCl_4$, $[(CH_3)_4Sb]_2ZnCl_4$ and $[(CH_3)_4Sb]_2CoBr_4$, $[(CH_3)_4Sb]_2CuBr_4$, $[(CH_3)_4Sb]_2ZnBr_4$, which have larger ratios of cation to anion radii, are grouped into a separate $[(CH_3)_4As]_2CoCl_4$ structure type, which is characterized by an apparent association with a cubic unit cell having ≈ 12.7 Å axes.

I. INTRODUCTION

The phase transitions of $[(CH_3)_4N]_2MX_4$ compounds, where M is Mn^{2+}, Fe^{2+}, Co^{2+}, Ni^{2+}, Cu^{2+}, or Zn^{2+} and X is Cl^-, Br^-, or I^-, have been extensively studied. The driving interest behind many of the studies has been the experimental search for, and the theoretical understanding of, transitions associated with incommensurately modulated phases. The characterized $[(CH_3)_4N]_2MX_4$ salts [hereafter $(TMA)_2MX_4$, where TMA= tetramethylammonium] all show transitions to a high-temperature, β-K_2SO_4 structure type[1,2] *Pmcn* phase with pseudohexagonal,[3] prototype axes of $a \approx 9$ Å, $b \approx \sqrt{3}\,a$ and $c \approx 13$ Å.[2,4–7] At lower temperatures these compounds show transitions to subgroup monoclinic or orthorhombic phases.[2,6–9] In this paper "β-K_2SO_4 structure type" includes both the structure of the *Pmcn* phase and the slightly perturbed subgroup structures. Thus all the characterized phases of all $(TMA)_2MX_4$ salts reported to date are grouped within this class. For these salts, first- and second-order phase transitions with distortions corresponding to the center ($\mathbf{k}=\mathbf{0}$) of the parent (*Pmcn*) Brillouin zone and along $\mathbf{b}^*$ (bromides and iodides) and $\mathbf{c}^*$ (chlorides) have been observed, with $\mathbf{k}\neq\mathbf{0}$ distortions including both incommensurate and commensurate modulations.

In an interesting extension of the $(TMA)_2MX_4$ family, deuterated analogs of several $(TMA)_2MX_4$ compounds have also been studied.[2] Deuteration of $(TMA)_2ZnCl_4$ perturbed the system enough to change the space group symmetry of one phase.[2] Following this idea of altering the quaternary organic cation, we have recently synthesized analogous salts in which the central nitrogen atom of the cation is replaced by higher members of the pnicogen group, P, As, and Sb. Two members of this newly extended family of $(TMZ)_2MX_4$ compounds, $(TMP)_2CuCl_4$ (Ref. 10) and $(TMP)_2CuBr_4$,[11] have been shown to be of the β-K_2SO_4 types. Both show phases similar in several respects to their ammonium analogues: $(TMP)_2CuCl_4$ and $(TMA)_2CuCl_4$ are modulated with wave vectors along $\mathbf{c}^*$ while $(TMP)_2CuBr_4$ and $(TMA)_2CuBr_4$ are modulated with wave vectors along $\mathbf{b}^*$. However, while $(TMP)_2CuCl_4$ has an incommensurate phase, as does $(TMA)_2CuCl_4$, $(TMP)_2CuBr_4$ does not, in contrast to $(TMA)_2CuBr_4$.

The results for two other members of the extended $(TMZ)_2MX_4$ family, $(TMAs)_2CoCl_4$ and $(TMAs)_2ZnCl_4$, have also been reported.[12] They are isomorphic at room temperature, but, in sharp contrast to the symmetries of the β-K_2SO_4 type structures discussed above, have $P4_2/mbc$ space group symmetry. Single crystal x-ray structure analyses confirmed the distinction, indicating structures quite different from the β-K_2SO_4 type.

In this work we continue our phase transition studies of the extended $(TMZ)_2MX_4$ family, introducing another 16 analogs (Z = P, As, Sb; M = Co, Cu, Zn; and X = Cl, Br, I) of previously reported $(TMA)_2MX_4$ compounds. Experimental details concerning the synthesis, chemical and IR spectroscopic characterizations, and techniques of other physical measurements are presented in Sec. II. A review and correlation using Landau theory of characterized $(TMA)_2MX_4$ salts and the two recently reported $(TMP)_2CuX_4$ compounds (all with the β-K_2SO_4 structure type) are presented in Sec. III. The discussion of the experimental results for the 16 new compounds is presented in Sec. IV. The compounds are discussed according to their structure, either in terms of the familiar β-K_2SO_4 type or in terms of a new type, named after the $(TMAs)_2CoCl_4$ prototype mentioned above. Compounds in the first category are placed within the Landau frame-

work developed in Sec. III. Finally, simple empirical criteria are developed to predict the structure type adopted by a given $(TMZ)_2MX_4$ compound. Conclusions and a survey of ongoing and future work are contained in Sec. V.

II. EXPERIMENT

A. Reagents

Reagent grade metal halides were purchased and used without further purification ($CuCl_2$, $CuBr_2$, $CoCl_2 \cdot 6H_2O$, $ZnCl_2$, Baker; $CoBr_2 \cdot xH_2O$, CoI_2, Alfa; $ZnBr_2$, ZnI_2, Aldrich) except for the cobalt halide polyhydrates which were dehydrated in a vacuum oven before use.

$(CH_3)_3Z$ (Z=P,As,Sb) was prepared by reaction of ZCl_3 with methylmagnesium iodide, for Z=As, Sb, or methylmagnesium bromide, for Z=P, in diethyl ether with a 1:5 molar ratio between the *pn*icogen trichloride and the methyl Grignard. A molar excess of CH_3I was added to a freshly distilled, ethereal solution of trimethyl pnicogen. The white, solid product $(CH_3)_4ZI$ was then allowed to settle out over a period of two to three weeks. All preparations were carried out under an argon atmosphere.[13]

The lower halide salts (chloride and bromide) were prepared from the iodides by metathesis with the appropriate silver halide in water.[14] In some cases it was necessary to synthesize the higher halide salts from the lower halides. This was accomplished by a two-step metathesis:

$$2(CH_3)_4ZX + Ag_2O + H_2O \xrightarrow{H_2O} (CH_3)_4ZOH + 2AgX \ , \quad (1)$$

$$(CH_3)_4ZOH + HX' \xrightarrow{H_2O} (CH_3)_4ZX' + H_2O \ . \quad (2)$$

B. Synthesis

Salts with composition $[(CH_3)_4Z]_2MX_4$ (Z=P,As,Sb; X=Cl,Br; M=Co,Cu,Zn) were precipitated upon mixing an alcoholic solution of $(CH_3)_4ZX$ with an alcoholic solution of MX_2 in a 2:1 ratio of the cation halide to the metal halide. The washed and dried product was recrystallized from acetonitrile by slow evaporation. The bromide salts, for M=Co and Zn, appeared to incorporate the acetonitrile solvent into their lattice since the crystals became opaque on drying. However, the $[(CH_3)_4Z]_2MBr_4$ salts (Z=P,Sb; M=Co,Zn) can be successfully grown by slow evaporation from aqueous solution. The corresponding arsonium salts were not successfully crystallized from acetonitrile, water, or nitromethane, apparently incorporating solvent in each case and becoming opaque on drying.

The corresponding iodide salts for M=Co and Zn and Z=P and As were crystallized by slow evaporation from an aqueous solution of $(CH_3)_4ZI$ and MI_2 with a large (3 to 4 times) stoichiometric excess of MI_2. The solution must be filtered after dissolution of the reagents to remove any MI_2 decomposition products. Crystal growth of the $[(CH_3)_4Sb]_2MI_4$ salts (M=Co,Zn) was unsuccessful.

C. Metal analyses

The compounds were analyzed for M^{2+} spectrophotometrically. Cu^{2+} was complexed with EDTA and analyzed directly[15] while Zn^{2+} and Co^{2+} were complexed with dithizone and analyzed using the "monocolor" method.[15] % Found (% calculated): $(TMP)_2CoCl_4$—15.20 (15.39), $(TMP)_2CoBr_4$—10.34 (10.51), $(TMP)_2CoI_4$—not analyzed, $(TMAs)_2CoCl_4$—12.37 (12.52), $(TMAs)_2CoI_4$—6.96(7.04), $(TMSb)_2CoCl_4$—10.37 (10.44), $(TMSb)_2CoBr_4$—7.41 (7.94), $(TMSb)_2CoI_4$—not analyzed, $(TMP)_2ZnCl_4$—16.53 (16.79), $(TMP)_2ZnBr_4$—11.18 (11.53), $(TMP)_2ZnI_4$—8.27 (8.66), $(TMAs)_2ZnCl_4$—13.52 (13.70), $(TMAs)_2ZnI_4$—7.75 (7.48), $(TMSb)_2ZnCl_4$—11.42 (11.45), $(TMSb)_2ZnBr_4$—not analyzed, $(TMSb)_2ZnI_4$—not analyzed, $(TMP)_2CuCl_4$—16.28 (16.40), $(TMP)_2CuBr_4$—11.2 (11.5), $(TMAs)_2CuCl_4$—13.7 (13.4), $(TMAs)_2CuBr_4$—10.2 (9.7), $(TMSb)_2CuCl_4$—10.8 (11.2), $(TMSb)_2CuBr_4$—8.5 (8.5).

D. Cation characterizations

The $(TMP)^+$, $(TMAs)^+$, and $(TMSb)^+$ cations were characterized by infrared spectroscopy on a Perkin-Elmer 283B spectrometer. The samples were prepared as solid pellets with either KCl or KI. The observed frequencies between 300 and 4000 cm^{-1} are given in Table I. The normal mode assignments are based on Refs.

TABLE I. Infrared spectroscopy results (cm^{-1}). The range and relative intensities of (main) peaks for the observed modes in the $(TMZ)_2MX_4$ compounds (Z=P,As,Sb; M=Co,Cu,Zn; X=Cl,Br,I) are given.

	ν_{13}	ν_{10}	ν_{15}	ν_{16}	ν_{17}	ν_{18}
$(TMP)_2MX_4$	2986–2967 *s*	2914–2893 *m*	1435–1415 *m*	1308–1295 *m*	985–972 *vs*	778–769 *m*
$(TMAs)_2MX_4$	3008–2984 *s*	2918–2902 *w*	1428–1411 *m*	1272–1268 *w*	937–920 *vs*	644–640 *s*
$(TMSb)_2MX_4$	3007–2992 *m*	2925–2905 *w*	1419–1410 *m*	1223–1220 *w*	865–858 *vs*	567–560 *s*

16–18. Under the point group T_d, the IR-allowed vibrational modes belong to the T_2 (F_2) representation. Six of the seven cation T_2 modes are observed, the seventh is expected between ≈ 178 cm^{-1} ($TMSb^+$) (Ref. 18) and ≈ 288 cm^{-1} (TMP^+).[17] The observed frequencies of individual compounds are available as deposited material.[19]

E. Single crystal x-ray studies

The lattice parameters and intensity data were obtained on $P2_1$ (upgraded to $P3F$ specifications) and $R3m$ Nicolet/Siemens diffractometers with graphite monochromated Cu $K\alpha$ and Mo $K\alpha$ radiation. The lattice parameters were obtained from least-squares analysis of 25 high-angle reflections.[20] Sets of restricted range intensity data (incomplete shells) were collected by fast (60°/min) Wycoff-ω scans. These served primarily to provide high-angle centering reflections, but also served to verify space-group assignments for some compounds (see Sec. IV).

F. Differential scanning calorimetry

The temperatures and entropies of transition were obtained on a Perkin-Elmer DSC7 differential scanning calorimeter. Crystallized samples were ground and thermograms were obtained at 5°/min. Low-temperature data, up to 60 °C, were collected with liquid nitrogen as the coolant and were calibrated with the solid-solid phase transition at −87 °C and the melting transition at 7 °C of cyclohexane. High-temperature data, from 40 °C, were collected without coolant and were calibrated with the melting transitions of indium at 157 °C and lead at 327 °C. Most thermograms were repeated at least once, with new samples, enabling uncertainties to be estimated.

III. REVIEW AND LANDAU CORRELATION OF $(TMA)_2MX_4$ and $(TMP)_2CuX_4$ COMPOUNDS

Tanisaki and Mashiyama[21,22] and Hasebe *et al.*[23] have shown that the sub-*Pmcn* phases of $(TMA)_2ZnCl_4$ and $(TMA)_2CuBr_4$ may be considered as induced from single irreducible representations of *Pmcn*. This applies not only to the phases observed directly below the *Pmcn* phase, as required by Landau theory since the phase transition is continuous, but also to subsequent, lower temperature phases. Furthermore, they show that the different irreducible representations corresponding to the distortions leading to the various phases are, for each compound, compatible. Other authors have noted the same properties for sub-*Pmcn* phases of various other $(TMA)_2MX_4$ compounds.[9,24,25]

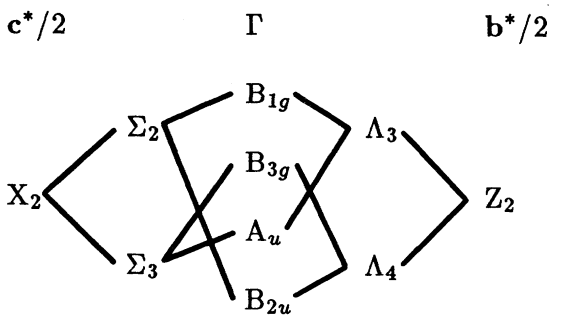

FIG. 1. Compatibility relations for irreducible representations of *Pmcn* along **b*** and **c***.

These observations may be combined and extended to all β-K_2SO_4 structure type $(TMZ)_2MX_4$ compounds. We note that the distortion representations of *Pmcn* for all characterized phases of β-K_2SO_4 types $(TMZ)_2MX_4$ compounds are compatible with either X_2 at **c***/2 or Z_2 at **b***/2. The compatibility relations are combined in Fig. 1. A correlation of the labels used in this paper with those employed by other authors[21,23,26–29] is given in the Appendix. Our labels are those derived for axes corresponding to *Pnma*.[30] Modulation directions and lattice parameters refer, however, to the *Pmcn* orientation commonly used. Table II lists the possible low symmetry groups induced at X, Γ, Z, and various points between, again only considering representations compatible with X_2 and Z_2. Table III gives the phases and representations of the distortions inducing, and hence the symmetries of, the known phases of β-K_2SO_4 type $(TMZ)_2MX_4$ (Z=N,P; M=Mn,Fe,Co,Ni,Cu,Zn; X=Cl,Br,I; hydrogenated or deuterated) compounds at one atmosphere.[2,6–8,26,31–35] Table IV includes the associated entropies and temperatures of transition[4–6,26,33,36–46] for the hydrogenated salts with

TABLE II. Space groups and superspace groups as induced from *Pmcn* for selected points of the Brillouin zone. For the two-dimensional representations, corresponding to $\mathbf{k}\neq 0$, the phase of the distortion is given by a superscript (arb = arbitrary).

k	Distortion representation and induced (super)space group			
c*/2	$X_2^0 \rightarrow P2_1/c11$	$X_2^{\pi/2} \rightarrow Pc2_1n$	$X_2^{\neq 0,\pi/2} \rightarrow Pc11$	
2**c***/5	$\Sigma_2^0 \rightarrow P12_1/c1$	$\Sigma_2^{\pi/2} \rightarrow P2_1cn$	$\Sigma_2^{\neq 0,\pi/2} \rightarrow P1c1$	
	$\Sigma_3^0 \rightarrow P112_1/n$	$\Sigma_3^{\pi/2} \rightarrow P2_12_12_1$	$\Sigma_3^{\neq 0,\pi/2} \rightarrow P112_1$	
c*/3	$\Sigma_2^0 \rightarrow P112_1/n$	$\Sigma_2^{\pi/2} \rightarrow P2_12_12_1$	$\Sigma_2^{\neq 0,\pi/2} \rightarrow P112$	
	$\Sigma_3^0 \rightarrow P12_1/c1$	$\Sigma_3^{\pi/2} \rightarrow P2_1cn$	$\Sigma_3^{\neq 0,\pi/2} \rightarrow P1c1$	
γ**c***, $0<\gamma<\frac{1}{2}$[a]	$\Sigma_2^{arb} \rightarrow P(Pmcn):(s1\bar{1})$		$\Sigma_3^{arb} \rightarrow P(Pmcn):(ss\bar{1})$	
0	$B_{1g} \rightarrow P12_1/c1$	$B_{3g} \rightarrow P112_1/n$	$A_u \rightarrow P2_12_12_1$	$B_{2u} \rightarrow P2_1cn$
β**b***, $0<\beta<\frac{1}{2}$[a]	$\Lambda_3^{arb} \rightarrow P(Pmcn):(s\bar{1}s)$		$\Lambda_4^{arb} \rightarrow P(Pmcn):(s\bar{1}1)$	
b*/2	$Z_2^0 \rightarrow P2_1/b11$	$Z_2^{\pi/2} \rightarrow Pbc2_1$	$Z_2^{\neq 0,\pi/2} \rightarrow Pb11$	

[a]Incommensurate.

TABLE III. The distortion representations of *Pmcn* (phase I) inducing the known phases of the β-K_2SO_4 structure type $(TMZ)_2MX_4$ (Z=N,P,As; M=Mn,Fe,Co,Ni,Cu,Zn; X=Cl,Br,I) compounds. Roman numerals II through VI refer to sequentially lower temperature phases specified in Table IV and elsewhere (Refs. 2 and 7).

Compound	Phase II	III	IV	V	VI
$(TMA)_2MnCl_4$[a,b]	$\Sigma_{2or3}^{arb}(\gamma\mathbf{c}^*)$	$X_2^0\left[\frac{\mathbf{c}^*}{2}\right]$	$\Sigma_2^0\left[\frac{\mathbf{c}^*}{3}\right]$	$B_{1g}(\mathbf{0})$	
$(TMA)_2FeCl_4$[a,b]	$\Sigma_{2or3}^{arb}(\gamma\mathbf{c}^*)$	$X_2^0\left[\frac{\mathbf{c}^*}{2}\right]$	$\Sigma_2^0\left[\frac{\mathbf{c}^*}{3}\right]$		
$(TMA)_2CoCl_4$[a,c]	$\Sigma_2^{arb}(\gamma\mathbf{c}^*)$[d]	$\Sigma_2^{\pi/2}\left[\frac{2\mathbf{c}^*}{5}\right]$	$\Sigma_2^0\left[\frac{\mathbf{c}^*}{3}\right]$	$B_{1g}(\mathbf{0})$	$\Sigma_2^{\pi/2}\left[\frac{\mathbf{c}^*}{3}\right]$
$(TMA)_2NiCl_4$[b,e]	$\Sigma_{2or3}^{arb}(\gamma\mathbf{c}^*)$	$X_2^0\left[\frac{\mathbf{c}^*}{2}\right]$	$B_{1g}(\mathbf{0})$		
$(TMA)_2CuCl_4$[b,f]	$\Sigma_3^{arb}(\gamma\mathbf{c}^*)$	$\Sigma_3^0\left[\frac{\mathbf{c}^*}{3}\right]$	$B_{3g}(\mathbf{0})$		
$(TMA)_2ZnCl_4$[a,g]	$\Sigma_2^{arb}(\gamma\mathbf{c}^*)$	$\Sigma_2^{\pi/2}\left[\frac{2\mathbf{c}^*}{5}\right]$	$\Sigma_2^0\left[\frac{\mathbf{c}^*}{3}\right]$	$B_{1g}(\mathbf{0})$	$\Sigma_2^{\pi/2}\left[\frac{\mathbf{c}^*}{3}\right]$
d$(TMA)_2CoCl_4$[a,b]	$\Sigma_2^{arb}(\gamma\mathbf{c}^*)$	$\Sigma_2^{\pi/2}\left[\frac{2\mathbf{c}^*}{5}\right]$	$\Sigma_2^0\left[\frac{\mathbf{c}^*}{3}\right]$	$B_{1g}(\mathbf{0})$	$\Sigma_2^{\pi/2}\left[\frac{\mathbf{c}^*}{3}\right]$
d$(TMA)_2ZnCl_4$[a,b]	$\Sigma_2^{arb}(\gamma\mathbf{c}^*)$	$X_2^0\left[\frac{\mathbf{c}^*}{2}\right]$[h]	$\Sigma_2^0\left[\frac{\mathbf{c}^*}{3}\right]$	$B_{1g}(\mathbf{0})$	$\Sigma_2^{\pi/2}\left[\frac{\mathbf{c}^*}{3}\right]$
$(TMP)_2CuCl_4$[i]	$\Sigma_3^{arb}(\gamma\mathbf{c}^*)$	$\Sigma_3^0\left[\frac{\mathbf{c}^*}{3}\right]$			
$(TMA)_2MnBr_4$[a]	$B_{1g}(\mathbf{0})$				
$(TMA)_2CoBr_4$[a]	$B_{1g}(\mathbf{0})$				
$(TMA)_2CuBr_4$[j]	$\Lambda_4^{arb}(\beta\mathbf{b}^*)$	$Z_2^{\pi/2}\left[\frac{\mathbf{b}^*}{2}\right]$	$B_{1g}(\mathbf{0})$		
$(TMA)_2ZnBr_4$[a]	$B_{1g}(\mathbf{0})$				
$(TMP)_2CoBr_4$[b]	$B_{1g}(\mathbf{0})$				
$(TMP)_2CuBr_4$[k]	$Z_2^0\left[\frac{\mathbf{b}^*}{2}\right]$				
$(TMP)_2ZnBr_4$[b]	$B_{1g}(\mathbf{0})$				
$(TMA)_2ZnI_4$[l]	$B_{1g}(\mathbf{0})$	$Z_2^{\pi/2}\left[\frac{\mathbf{b}^*}{2}\right]$			
$(TMP)_2CoI_4$[b]	$B_{1g}(\mathbf{0})$				
$(TMP)_2ZnI_4$[b]	$B_{1g}(\mathbf{0})$				
$(TMAs)_2CoI_4$[b]	$B_{1g}(\mathbf{0})$				
$(TMAs)_2CuBr_4$[b]	$Z_2^0\left[\frac{\mathbf{b}^*}{2}\right]$				
$(TMAs)_2ZnI_4$[b]	$B_{1g}(\mathbf{0})$				

[a]Reference 2.
[b]This study.
[c]Reference 32.
[d]Includes both the II and II′ phases (II′ is the reentrant incommensurate phase occurring between phases III and IV).
[e]Reference 7.
[f]Reference 33.
[g]References 26 and 35.
[h]Phase is only occasionally observed, see Ref. 2.
[i]Reference 10.
[j]References 8 and 34.
[k]Reference 11.
[l]Reference 6.

TABLE IV. $(TMZ)_2MX_4$ (Z=N,P,As,Sb; M=Co,Cu,Zn; X=Cl,Br,I) temperatures (K) and entropies ($\Delta S/R$) of transition. Estimated uncertainties in parentheses. Format is $T_{tr}/\Delta S_{tr}$. Columns are headed by the central Z atom of the cation. Blocks of data corresponding to phase sequences of individual compounds are headed by the temperature range (K) of the experiment. Underlined numbers indicate continuous and/or λ-shaped transitions. Highest temperature transitions separate phases I and II, etc.

Anion	N	P	As	Sb
	(60–330)[a,c]	(103–523)[b,d]	(113–573)[b,d,e]	(113–523)[b,d]
$CoCl_4$	**294.0(2)/1.06(5)**	465(1)/1.8(2)	**545(1)/0.29(3)**	475.0(7)/0.9(1)
	282.35(10)/0.012(4)	322(1)/1.3(2)	339(1)/0.87(9)	
	277.65(10)/0.037(2)[f]			
	191.9(5)/0.295(4)			
	115.9(5)/0.18(5)			
	(93–308)[a,g]	(113–523)[a,d]		(113–523)[b,d]
$CoBr_4$	**287.0/?**	**366.8(8)/1.1(2)**		452(1)/1.5(2)
		(103–523)[a,d]	(113–523)[a,d]	
CoI_4		**376.0(6)/1.1(2)**	**398(1)/1.7(3)**	
	(50–327)[a,h]	(103–483)[a,d,i]	(113–523)[b,d]	(113–493[j])[b,d]
$CuCl_4$	**298.79(2)/0.49(5)**	**380.4(5)/0.4(2)**	**487.8(7)/0.42(8)**	490(1)/0.7(4)
	2928(2)/0.008(2)	346.3(6)/0.14(2)	260(1)/0.7(1)	408.2(7)/0.9(1)
	264.82(3)/0.261(5)			160(1)/0.28(5)
				140(1)/1.0(2)
	(60–343)[a,k]	(113–593)[a,d,l]	(113–523)[a,d]	(103–488[j])[b,d]
$CuBr_4$	**270.70(5)/0.49(5)**	**406.2(8)/0.9(1)**	**405.7(7)/1.3(2)**	**478(1)/0.3(1)**
	249.35(5)/0.008(2)	196(1)/0.4(2)	266(1)/0.72(8)	359.4(8)/1.0(1)
	242.80(5)/0.261(5)			177.5(8)/0.9(2)
	(48–330)[a,m]	(103–573)[b,d]	(103–573)[b,d,e]	(103–523)[b,d]
$ZnCl_4$	**296.65(5)/1.2(6)**	460(1)/2.3(3)	**550(1)/0.35(8)**	459.8(8)/0.9(1)
	280.95(5)/0.007(3)	317(1)/1.5(2)	335.9(8)/1.0(1)	
	277.40(6)/0.0375(5)			
	170.65(6)/0.232(7)[n]			
	159.01(6)/0.132(15)			
	(100–316)[a,o]	(113–523)[a,d]		(103–523)[b,d]
$ZnBr_4$	**288/0.98**	**368.7(8)/1.1(3)**		446(1)/1.5(2)
	(4.2–293)[a,p]	(103–523)[a,d]	(113–523)[a,d]	
ZnI_4	**254/?**	**378(1)/1.2(4)**	**405.4(8)/1.6(3)**	
	210/?			

[a] β-K_2SO_4 structure type.
[b] $[(CH_3)_4As]_2CoCl_4$ structure type.
[c] References 36, 44, and 45.
[d] This study.
[e] Reference 12.
[f] This reported data apparently spans two transitions which bracket a reentrant incommensurate phase, referred to as II′ in Table III.
[g] Reference 46.
[h] References 5 and 37.
[i] Reference 10.
[j] Oxidized.
[k] Reference 38.
[l] Reference 11.
[m] References 26, 36, 39, and 40.
[n] Corresponds to $\Delta S_{IV\text{-}V} + \Delta S_{V\text{-}VI}$ in Ref. 39. See also Ref. 26 and references therein.
[o] References 4 and 41–43.
[p] References 6 and 33.

M=Co, Cu, and Zn only. Phase transition entropies are unavailable for the salts with M=Mn, Fe, and Ni, or for any deuterated analogs; only their transition temperatures have been reported.[2,7]

Superspace groups,[47] used to describe modulated structures, are also listed in Tables II and III. The superspace group assignments for the incommensurate phase of several $(TMA)_2MCl_4$ salts, where M=Mn, Fe, Ni, and Cu, or the deuterated salts, where M=Co and Zn, have not been previously reported. The superspace group $P(Pmcn):(ss\bar{1})$ is assigned to $(TMA)_2CuCl_4$ and $P(Pmcn):(s1\bar{1})$ is assigned to $d(TMA)_2CoCl_4$ in a manner identical to one applied to K_2SeO_4.[48,49] This assumes the symmetry of the distortion remains compatible through the lock-in transition. By similar analysis, the possible superspace groups for phase II of the Mn, Fe, Ni, and the deuterated Zn analogs may be reduced to the same two groups. As mentioned above, distortion symmetries are expected to remain compatible over the entire sub-*Pmcn* phase sequence for a given β-K_2SO_4 type $(TMZ)_2MX_4$ salt so the correct superspace group assignment for all four analogs is almost certainly $P(Pmcn):(s1\bar{1})$. This could be verified by analyzing first-order satellite reflections. Extinction conditions for $P(Pmcn):(ss\bar{1})$ differ from those for $P(Pmcn):(s1\bar{1})$ only for $(h0lm)$ reflections: $l+m$=odd implies the former group and l=odd implies the latter group.

Another empirical criterion concerning sub-*Pmcn* space group assignments of $(TMZ)_2MX_4$ salts can be made by correlating the symmetries of the phase transition distortions with the requirments of Landau theory for continuous transitions. In other words, an effective Landau theory (ignoring the Lifschitz criterion[50]) seems to apply in which intervening phases between the prototype *Pmcn* phase and the phase of interest may be ignored and one can pretend that the transition to the phase of interest occurs directly from the *Pmcn* phase, and is continuous. Thus we note that the distortion representations of Fig. 1 or Tables II and III are active[50] and further, the sub-*Pmcn* space groups (not superspace groups) of $(TMZ)_2MX_4$ compounds correspond to maximal isotropy groups in the relevant one- and two-dimensional irreducible representation spaces.[50] The distortions in Table II leading to nonmaximal isotropy groups are those with phases unequal to zero or $\pi/2$.

The derivations of the induced groups at $\mathbf{k}=\mathbf{c}^*/3$ and the superspace groups at $\mathbf{k}=\gamma\mathbf{c}^*$ are available as deposited material.[19]

IV. RESULTS AND DISCUSSION

The phase transitions and room-temperature lattice parameters of 16 new members of the $(TMZ)_2MX_4$ (Z=P, As, Sb; M=Co, Cu, Zn; X=Cl, Br, I), series of compounds have been determined. The differential scanning calorimetry results for this series are given in Table IV, as well as the data for the corresponding $Z=N$ members. Table V reports room-temperature lattice parameters and, in some cases, space groups for the 20 P, As, and Sb analogs only.

The discussion of the calorimetric and diffraction data of the 16 additional Z=P, As, and Sb members that follows will be separated into three segments. The first section deals with the seven β-K_2SO_4 type compounds, the second section deals the remaining nine compounds, all of which are grouped into a new category named after the $(TMAs)_2CoCl_4$ prototype, and the final section provides empirical criteria categorizing all $(TMZ)_2MX_4$ salts by these structural types.

TABLE V. $(TMZ)_2MX_4$ (Z=P, As, Sb; M=Co, Cu, Zn; X=Cl, Br, I) room-temperature x-ray diffraction results.

Compound	Bravais lattice/ space group	Lattice parameters a(Å)	b(Å)	c(Å)	α or β	Z	Ref.
$(TMP)_2CoCl_4$	Orthorhombic P	12.758(3)	18.385(2)	25.134(3)		12	
$(TMAs)_2CoCl_4$	$P4_2/mbc$	17.831(2)		25.20(1)		16	12
$(TMSb)_2CoCl_4$	Cubic F	25.112(2)				32	
$(TMP)_2CoBr_4$	$P12_1/c1$	9.489(2)	15.985(3)	13.106(2)	90.48(2)	4	
$(TMSb)_2CoBr_4$	Cubic F	25.882(7)				32	
$(TMP)_2CoI_4$	$P12_1/c1$	9.865(3)	16.767(4)	13.726(2)	90.07(2)	4	
$(TMAs)_2CoI_4$	$P12_1/c1$	9.960(2)	16.716(2)	13.747(2)	90.29(1)	4	
$(TMP)_2CuCl_4$	$P12_1/c1$	9.251(3)	15.569(5)	37.581(12)	90.23(3)	12	10
$(TMAs)_2CuCl_4$	Tetragonal I	12.464(2)		25.342(6)		8	
$(TMSb)_2CuCl_4$	Cubic F	25.022(6)				32	
$(TMP)_2CuBr_4$	$P2_1/b11$	9.496(5)	31.600(6)	13.038(7)	90.33(3)	8	11
$(TMAs)_2CuBr_4$	$P2_1/b11$	9.604(3)	31.936(9)	13.062(5)	90.92(3)	8	
$(TMSb)_2CuBr_4$	Cubic F	25.889(3)				32	
$(TMP)_2ZnCl_4$	Orthorhombic P	12.754(2)	18.360(2)	25.100(4)		12	
$(TMAs)_2ZnCl_4$	$P4_2/mbc$	17.820(1)		25.209(3)		16	12
$(TMSb)_2ZnCl_4$	Cubic F	25.103(2)				32	
$(TMP)_2ZnBr_4$	$P12_1/c1$	9.502(3)	16.013(2)	13.114(3)	90.47(2)	4	
$(TMSb)_2ZnBr_4$	Cubic F	25.967(3)				32	
$(TMP)_2ZnI_4$	$P12_1/c1$	9.880(2)	16.785(2)	13.728(2)	90.05(2)	4	
$(TMAs)_2ZnI_4$	$P12_1/c1$	9.960(2)	16.716(2)	13.747(2)	90.29(1)	4	

A. β-K_2SO_4 type compounds

The 16 compounds marked with footnote a in Table IV have axial lengths which are either of the *Pmcn* β-K_2SO_4 prototype, $a \approx 9$ Å, $b \approx \sqrt{3}\,a$, and $c \approx 13$ Å, or else equal to a small multiple of these lengths. Of these, x-ray crystal structure analyses of $(TMA)_2CoCl_4$, $(TMA)_2CuCl_4$, $(TMA)_2ZnCl_4$, $(TMA)_2CuBr_4$, $(TMA)_2ZnBr_4$, $(TMA)_2ZnI_4$, and $(TMP)_2CuBr_4$ have been done, indicating that all seven have the β-K_4SO_4 type structure. $(TMA)_2CoBr_4$ is also believed to have this structure type.[2] The similarity of lattice parameters and the evidence from DSC experiments (see below) show that the other eight compounds, $(TMP)_2CuCl_4$, $(TMP)_2CoBr_4$, $(TMP)_2ZnBr_4$, $(TMP)_2CoI_4$, $(TMP)_2ZnI_4$, $(TMAs)_2CoI_4$, $(TMAs)_2CuBr_4$, and $(TMAs)_2ZnI_4$, also have β-K_2SO_4 type structures.

The P, As, and Sb analogs, as all of the previously studied $(TMA)_2MX_4$ compounds, have, as a common feature, a λ shaped and/or continuous high-temperature transition, as is noted in Table IV. By λ shaped, we mean the DSC scans show a definite low-temperature tail. For the $Z=N$ salts, and for $(TMP)_2CuCl_4$ and $(TMP)_2CuBr_4$, this I-II transition has been shown to separate the prototype *Pmcn* phase from a subgroup or incommensurate phase.[2,10,11] Generalizing to the seven new β-K_2SO_4 type P, As, and Sb compounds, $(TMP)_2CoBr_4$, $(TMP)_2ZnBr_4$, $(TMP)_2CoI_4$, $(TMP)_2ZnI_4$, $(TMAs)_2CuBr_4$, $(TMAs)_2CoI_4$, and $(TMAs)_2ZnI_4$, *Pmcn* symmetry is also probable above this transition. The β-K_2SO_4 type P, As, and Sb compounds are all monoclinic at room temperature, corresponding to a ferroelastic distortion of the orthorhombic phase. As expected, slight pressure was enough to form easily movable twin domains in these crystals, which were observed using polarized-light microscopy.

The room temperature, phase-II space groups of the β-K_2SO_4 type P, As, and Sb analogs are given explicitly in Table V, or can be obtained indirectly from Tables II, III, and IV. The experimentally obtained x-ray diffraction intensity data of the seven new β-K_2SO_4 type P, As, and Sb analogs were of limited range and accuracy (see Sec. II) and were not considered sufficient to definitively determine 2_1 screw axis symmetry elements. However, since the DSC results point toward (nearly) continuous I-II transitions, Landau theory was invoked to complete the space group assignments. Phase-II lattice parameters of the new β-K_2SO_4 type P, As, and Sb analogs show that the relevant points of the primitive orthorhombic Brillouin zone are Γ [$(TMP)_2MBr_4$, $(TMP)_2MI_4$, and $(TMAs)_2MI_4$, $M=Co,Zn$] and Z [$(TMAs)_2CuBr_4$]. For the Γ point, the eight possible induced space groups include the four from Table II plus $A_g \rightarrow Pmcn$ (not active), $B_{2g} \rightarrow P2_1/m\,11$, $B_{1u} \rightarrow Pm2_1n$, and $B_{3u} \rightarrow Pmc2_1$. $(TMP)_2MBr_4$, $(TMP)_2MI_4$, and $(TMAs)_2MI_4$ ($M=Co,Zn$) have monoclinic unit cells with the **b** axis unique. Thus the logical choice of space group for phase II of these compounds is $P12_1/c1$. The systematic absences are in agreement, so the $P12_1/c1$ space group assignment is considered definitive. At Z, the six possible induced space groups are the three from Table II plus $Z_1^0 \rightarrow P2_1/m\,11$, $Z_1^{\pi/2} \rightarrow Pmc2_1$, and $Z_1^{\neq 0,\pi/2} \rightarrow Pm\,11$. The lattice parameters and systematic extinctions from intensity data for $(TMAs)_2CuBr_4$ indicated either $P2_1/b\,11$ or $Pb\,11$. No x-ray data were collected with $(h,0,0)$, $h=$odd indices however, so the 2_1 axis could not be assigned from systematic extinctions. However, Landau theory eliminates the $Pb\,11$ possibility since it does not correspond to a maximal isotropy group in the two-dimensional parameter space.[50] Thus, the $P2_1/b\,11$ space group assignment is considered correct.

The space groups for these seven β-K_2SO_4 type P, As, and Sb analogs, $P12_1/c1$ and $P2_1/b11$, are common to previously reported β-K_2SO_4 type $(TMZ)_2MX_4$ compounds (see Tables II and III). Thus the comments in Sec. III regarding common properties of distortion symmetries holds also for these compounds. In particular, the distortion representations are compatible with X_2 and Z_2. We know of no theoretical reason why X_1 and Z_1 compatible distortions should be excluded.

Except for $(TMP)_2CuCl_4$, there are probably no incommensurate phases in the β-K_2SO_4 type P, As, and Sb compounds. $(TMP)_2CuCl_4$ and $(TMA)_2MX_4$ compounds which have incommensurate phases have all shown a transition directly from the *Pmcn* prototype phase to an incommensurate phase. All of the additional, β-K_2SO_4 type compounds showed only one (continuous or nearly continuous, I-II) transition above room temperature as is indicated in Table IV. The x-ray analyses of these compounds at room temperature showed no incommensurate satellites. Thus, incommensurate phase are effectively ruled out for $(TMP)_2MBr_4$, $(TMP)_2MI_4$, and $(TMAs)_2MI_4$ ($M=Co,Zn$) which have only the one high-temperature transition. Phase III of $(TMP)_2CuBr_4$ and phase III of $(TMAs)_2CuBr_4$ probably have the symmetry of $Pbc2_1$ or one of the space groups induced at the Γ point, listed in Table II, and are not incommensurate. It is possible our DSC experiments have missed very weak transitions between room temperature and the high temperature, I-II transitions. Assuming this is not so, Table III, with Table II, gives all of the incommensurate phases of the listed β-K_2SO_4 type $(TMZ)_2MX_4$ compounds.

B. $(TMAs)_2CoCl_4$ type compounds

The remaining 11 $(TMZ)_2MX_4$ compounds in Table IV, indicated by footnote b, have orthorhombic, tetragonal, or cubic unit cells with non-β-K_2SO_4 prototype axes. Of these, the crystal structures of $(TMA)_2CoCl_4$ and $(TMAs)_2ZnCl_4$ have been reported.[12] As is mentioned in Sec. I their structures and space-group symmetries exclude them from the β-K_2SO_4 classification. Examination of the axial lengths of the 11 compounds shows an apparent structural correlation. The axes are always either ≈ 12.7 Å, or else $\approx\sqrt{2}$ or ≈ 2 times this length. Thus, all 11 salts are classified together in this paper as being of the $(TMAs)_2CoCl_4$ structure type.

X-ray analyses show no incommensurate satellites at room temperature for the 11 $(TMAs)_2CoCl_4$ structure type compounds. Incommensurate phases are unlikely for most of these compounds over any temperature range

as only $(TMAs)_2MCl_4$ with $M=Co,Cu,Zn$ and $(TMSb)_2CuBr_4$ have lambda-shaped, high temperature, I-II transitions. $(TMSb)_2CuCl_4$ shows a IV-V transition at 140 K which has a questionable lambda shape. X-ray studies of phase II of $(TMAs)_2CoCl_4$ showed satellite reflections attributable to either twinning or incommensurate modulation.[12] $(TMAs)_2CoCl_4$ is reported to have the symmetry of $I4_1/a$ with $a=12.61$ Å and $c=25.44$ Å at higher temperatures of its phase II.[12] Considering the similar I centered tetragonal unit cell of phase II of $(TMAs)_2CuCl_4$ at room temperature (Table V), along with the calorimetric data for both compounds from Table IV, it is apparent that $(TMAs)_2CoCl_4$ and $(TMAs)_2CuCl_4$ are either isomorphic and isostructural over their observed phase sequences or at least very similar. Thus, the absence of satellite reflections for $(TMAs)_2CuCl_4$ at room temperature seems to contradict the reported possible incommensurate results for $(TMAs)_2CoCl_4$. A crystallographic analysis of the room-temperature structure of $(TMAs)_2CuCl_4$, in progress, should determine the possible isomorphism of phase II of these two compounds and may clarify whether phase II of $(TMAs)_2CoCl_4$ is actually incommensurately modulated or merely twinned.

C. Criteria determining $(TMZ)_2MX_4$ structure types

The structure type adopted by a given $(TMZ)_2MX_4$ compound, either β-K_2SO_4 or $(TMAs)_2CoCl_4$, can be correlated with the ratio of Z-C to M—X bond lengths and the geometry of the anion. Since intraionic bond lengths for $(TMZ)_2MX_4$ salts should be only weakly perturbed by varying crystal symmetry, structure type, or even counterions, a plot of (expected) Z-C versus (expected) M—X bond lengths may be made for all $(TMZ)_2MX_4$ ($Z=N,P,As,Sb$; $M=Cu,Co,Zn$; $X=Cl,Br,I$) salts with data from only a few.[4-6,11,12,26,32,51] The results are presented in Figs. 2(a) and 2(b) for $M=Co$, Zn, and $M=Cu$, respectively. It is noted from these figures that $(TMZ)_2MX_4$ salts with smaller ratios of cation to anion radii form β-K_2SO_4 type structures while salts with larger ratios form the higher symmetry, $(TMAs)_2CoCl_4$ type structures. Indeed, for the $(TMAs)_2CoCl_4$ type structures, the larger the Z-C-to-M-X ratio, the higher the symmetry of the lattice. The salts with cubic symmetry [$(TMSb)_2MX_4$, $M=Co,Cu,Zn$, $X=Cl,Br$] have the largest ratios, those with tetragonal symmetry [$(TMAs)_2MCl_4$, $M=Co,Cu,Zn$] have intermediate, and those with orthorhombic symmetry [$(TMP)_2MCl_4$, $M=Co,Zn$] have the smallest ratios. The different structure types for $(TMP)_2CuCl_4$ versus $(TMP)_2MCl_4$ versus $(TMP)_2MCl_4$ ($M=Co,Zn$) compounds probably results from their different anion symmetries: tetragonally compressed CuX_4^{2-} tetrahedra versus regular CoX_4^{2-} and ZnX_4^{2-} tetrahedra.

V. FINAL REMARKS

This study of a broad range of $(TMZ)_2MX_4$ compounds has failed to unearth any extra compounds, besides $(TMP)_2CuCl_4$, that exhibit incommensurate behavior. Nevertheless, the negative results in this regard may help clarify parameters necessary for incommensurate behavior. Several compounds within this extended family fall into the β-K_2SO_4 structure type; their sub-*Pmcn* phases have been correlated in terms of Landau theory with other known compounds in this class. The universal compatibility of the distortion symmetries with either X_2 or Z_2 could perhaps be exploited in a generalized Landau free-energy expansion. The remainder of the compounds in the family belong to the new, and still not well-characterized, $(TMAs)_2CoCl_4$ structure type. The two structure types have been deliniated by the ratio of cation radius to anion radius. Thus it has become apparent why no $(TMZ)_2MX_4$ compound has been found with the new $(TMAs)_2CoCl_4$ structure.

We are currently pursuing several different lines of research within the $(TMZ)_2MX_4$ family. Single-crystal x-ray diffraction studies of the room-temperature phases

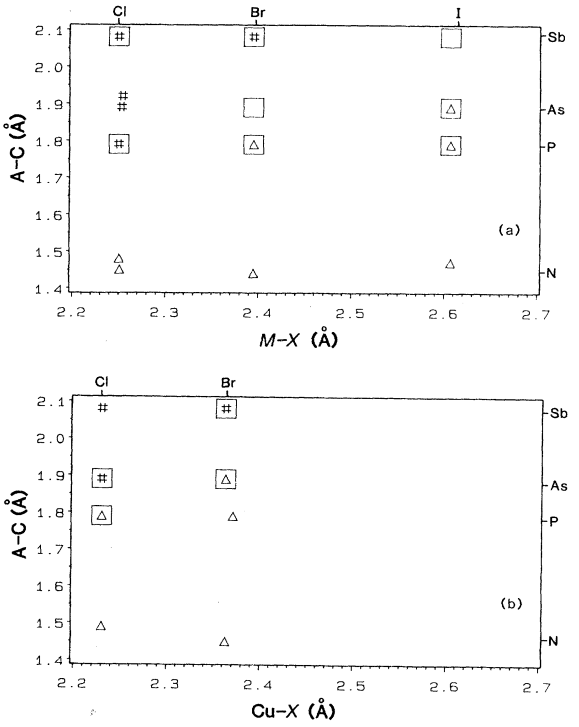

FIG. 2. Correlation of bond lengths in $(TMZ)_2MX_4$ salts with structural type. M in (a) represents Zn or Co and in (b) represents Cu. Triangles represent β-K_2SO_4 type structures and hash marks represent $(TMAs)_2CoCl_4$ type structures. Plotted bond lengths include the averaged, librationally uncorrected values for $(TMA)_2ZnCl_4$ [Ref. 26] (278 K), $(TMA)_2CoCl_4$ [Ref. 32] (280 K) $(TMA)_2ZnBr_4$ [Ref. 4] (293 K), $(TMA)_2ZnI_4$ [Ref. 6] (250 K), $(TMAs)_2CoCl_4$ [Ref. 12] (293 K), $(TMAs)_2ZnCl_4$ [Ref. 12] (293 K), $(TMA)_2CuCl_4$ [Ref. 5] (293 K), $(TMA)_2CuBr_4$ [Ref. 4] (293 K), $(TMP)_2CuBr_4$ [Ref. 11] (293 K), and $(TMSb)_2CuCl_4$ [Ref. 51] (293 K). A triangle or hash mark with a surrounding box represents expected bond lengths taken directly from the above structures. The size of the box is an estimate of the uncertainty in the expected librationally uncorrected bond lengths. An empty box represents an unsynthesized compound.

of the β-K_2SO_4 compounds $(TMP)_2CoBr_4$ and $(TMP)_2CoI_4$ are in progress. In regard to $(TMP)_2CuCl_4$, the one incommensurate system found in the extended family, single-crystal x-ray structures in the commensurate, incommensurate, and disordered phases are in progress. Also, a study of the temperature variation of the lattice constants and an adiabatic calorimetry study are underway in an effort to obtain numerical values for the Landau free-energy coefficients. Single-crystal x-ray structures are also underway for the $(TMAs)_2CoCl_4$ type compounds $(TMP)_2CoCl_4$, $(TMAs)_2CuCl_4$, $(TMSb)_2CuCl_4$, and $(TMSb)_2ZnBr_4$. Initial results indicate less similarity among these salts than has been observed in the β-K_2SO_4 group. Thus, while a Landau correlation may not apply for the new $(TMAs)_2CoCl_4$ type structures, structural correlations may still be found through simple descent of symmetry analysis.

ACKNOWLEDGMENTS

The x-ray-diffraction facility was established through funds from the National Science Foundation Grant No. CHE-840840, the Boeing Corporation, and Washington State University. We thank Tork Will for synthesis and IR assistance, and we also thank Professor Pérez-Mato for a critical reading of the manuscript.

APPENDIX

Correspondence between representation labels used by various authors for space group *Pnma* (standard setting).

Ref.	Correspondence between labels										Space group symbol
This work	X_2	Σ_2	Σ_3	B_{1g}	B_{3g}	A_u	B_{2u}	Λ_3	Λ_4	Z_2	*Pmcn*
21	Z_2	Λ_4	Λ_2	Γ_5	Γ_7	Γ_2	Γ_4				*Pmcn*
23				B_{2g}	B_{1g}	A_u	B_{3u}	Δ_2	Δ_4	Y_2	*Pmcn*
26		Σ_3	Σ_2								*Pmcn*
27	X_2	Σ_4	Σ_2	B_{1g}	B_{3g}	A_u	B_{2u}				*Pnma*
28	X_2	Σ_3	Σ_2	B_{2g}	B_{3g}	A_u	B_{1u}				*Pnam*
29		$T_1^{(k,4)}$	$T_1^{(k,2)}$	B_{1g}	B_{2g}	A_u	B_{3u}				*Pmnb*

[1]O. Muller and R. Roy, *The Major Ternary Structural Families* (Springer, New York, 1974).
[2]R. Perret, G. Godefroy, and H. Arend, Ferroelectrics **73**, 87 (1987) and references therein.
[3]H. Arnold, W. Kurtz, A. Richter-Zinnius, and J. Bethke, Acta Crystallogr. B **37**, 1643 (1981).
[4]P. Trouélan, J. Lefebvre, and P. Derollez, Acta Crystallogr. C **40**, 386 (1984).
[5]R. Clay, J. Murray-Rust, and P. Murray-Rust, Acta Crystallogr. B **31**, 289 (1975).
[6]K. Hasebe, T. Asahi, and K. Gesi, Acta Crystallogr. C **46**, 218 (1990) and reference therein.
[7]H. Kasano and H. Mashiyama, J. Phys. Soc. Jpn. **58**, 3175 (1989).
[8]T. Asahi, K. Hasebe, and K. Gesi, J. Phys. Soc. Jpn. **57**, 4219 (1988).
[9]J. Sugiyama, M. Wada, A. Sawada, and Y. Ishibashi, J. Phys. Soc. Jpn. **49**, 1405 (1980).
[10]M. R. Pressprich, M. R. Bond, R. D. Willett, and M. A. White, Phys. Rev. B **39**, 3453 (1989).
[11]G. Madariaga, M. M. Alberdi, and F. J. Zúñiga, Acta Crystallogr. C **43**, 2363 (1991).
[12]F. J. Zúñiga, M. J. Cabezudo, G. Madariaga, M. R. Pressprich, M. R. Bond, and R. D. Willett, Acta Crystallogr. B (to be published).
[13]H. Rager and A. Weiss, Z. Phys. Chem. **93**, 299 (1974).
[14]T. T. Ang and B. A. Dunell, J. Chem. Soc. Faraday Trans. **75**, 169 (1979).
[15]Z. Marczenko, in *Separation and Spectrophotometric Determination of Elements,* translation editor M. Masson (E. Horwood, Chichester; Halsted Press, New York, 1986).
[16]R. W. Berg, Spectrochim. Acta **34A**, 655 (1978).
[17]G. Tatzel, H. Schrem, and J. Weidlein, Spectrochim. Acta **34A**, 549 (1978).
[18]H. Siebert, Z. Anorg. Allg. Chem. **273**, 161 (1953).
[19]See AIP Document No. PAPS PRBMD-43-13 549-7 for seven pages of supplementary materials including complete IR results and the derivation of induced (super)space groups from *Pnma*. Order by PAPS number and journal reference from American Institute of Physics, Physics Auxiliary Publication Service, 335 East 45th Street, New York, N.Y. 10017. The prepaid price is $1.50 for a microfiche, or $5.00 for a photocopy. Airmail additional. Make checks payable to the American Institute of Physics.
[20]C. F. Campana, D. F. Shephard, and W. N. Litchman, Inorg. Chem. **20**, 4039 (1981).
[21]S. Taniasaki and H. Mashiyama, J. Phys. Soc. Jpn. **48**, 339 (1980).
[22]H. Mashiyama, J. Phys. Soc. Jpn. **49**, 2270 (1980).
[23]K. Hasebe, H. Mashiyama, and S. Tanisaki, J. Phys. Soc. Jpn. **53**, 2326 (1984).
[24]A. M. Fajidiga, J. Dolinšek, R. Blinc, A. P. Levanyuk, R. Perret, H. Arend, and R. Kind, Z. Phys. B **77**, 329 (1989).
[25]K. Hasebe, H. Mashiyama, S. Tanisaki, and K. Gesi, J. Phys. Soc. Jpn. **51**, 1045 (1982).
[26]G. Madariaga, F. J. Zúñiga, J. M. Pérez-Mato, and M. J. Tello, Acta Crystallogr. B **43**, 356 (1987).
[27]G. Marion, R. Almairac, M. Ribet, U. Steigenberger, and C.

Vettier, J. Phys. (Paris) **45**, 929 (1984).
[28]M. Iizumi, J. D. Axe, G. Shirane, and K. Shimaoka, Phys. Rev. B **15**, 4392 (1977).
[29]K. Parlinski and F. Dénoyer, J. Phys. C **18**, 293 (1985).
[30]C. J. Bradley and A. P. Cracknell, *The Mathematical Theory of Symmetry in Solids* (Clarendon, Oxford, England, 1972).
[31]B. Dam and A. Janner, Acta Crystallogr. B **42**, 69 (1986).
[32]E. Fjaer, Acta Crystallogr. B **41**, 330 (1985).
[33]K. Gesi and R. Perret, J. Phys. Soc. Jpn. **57**, 3698 (1988).
[34]G. Madariaga, F. J. Zúñiga, W. Paciorek, and E. Bocanegra, Acta Crystallogr. B (to be published).
[35]B. Dam and A. Janner, Acta Crystallogr. B **42**, 69 (1986).
[36]J. R. Wiesner, R. C. Srivastava, C. H. L. Kennard, M. DiVaira, and E. C. Lingafelter, Acta Crystallogr. **23**, 565 (1967).
[37]A. Gomez-Cuevas, M. J. Tello, J. Fernandez, A. López-Echarri, J. Herreros, and M. Couzi, J. Phys. C **16**, 473 (1983).
[38]A. López-Echarri, I. Ruiz-Larrea, and M. J. Tello, Phys. Status Solidi B **154**, 143 (1989).
[39]I. Ruiz-Larrea, A. López-Echarri, and M. J. Tello, J. Phys. C **14**, 3171 (1981).
[40]F. J. Zúñiga, G. Madariaga, and J. M. Pérez-Mato, Acta Crystallogr. B **45**, 462 (1989).
[41]R. Perret, Y. Beaucamps, G. Godefroy, P. Muralt, M. Ehrensperger, H. Arend, and D. Altermatt, J. Phys. Soc. Jpn. **52**, 2523 (1983).
[42]P. Trouélan, J. Lefebvre, and P. Derollez, Acta Crystallogr. C **41**, 846 (1985).
[43]T. Asahi, K. Hasebe, and K. Gesi, J. Phys. Soc. Jpn. **57**, 4219 (1988).
[44]A. Gomez-Cuevas, A. López-Echarri, M. J. Tello, and P. Vidaurrazaga, Ferroelectrics **36**, 339 (1981).
[45]K. Hasebe, H. Mashiyoma, and S. Tanisaki, J. Phys. Soc. Jpn. **51**, 2049 (1982).
[46]K. Gesi, J. Phys. Soc. Jpn. **51**, 203 (1982).
[47]P. M. DeWolff, T. Janssen, and A. Janner, Acta Crystallogr. A **37**, 625 (1981).
[48]J. M. Pérez Mato, G. Madariaga, and M. J. Tello, Ferroelectrics **53**, 293 (1984).
[49]J. M. Pérez-Mato, G. Madariaga, and M. J. Tello, Phys. Rev. B **30**, 1534 (1984).
[50]J. C. Tolédano and P. Toledano, *The Landau Theory of Phase Transitions* (World Scientific, Singapore, 1987).
[51]M. R. Pressprich, Ph.D. thesis, Washington State University.